Infrared properties of T'-phase R_2CuO_4 insulating compounds

S. L. Herr
Department of Physics, Virginia Commonwealth University, Richmond, Virginia 23284-2000

K. Kamarás
Central Research Institute of Physics, H1525 Budapest, Hungary

D. B. Tanner, S-W. Cheong,* and G. R. Stewart
Department of Physics, University of Florida, Gainesville, Florida 32611

Z. Fisk
Los Alamos National Laboratory, Los Alamos, New Mexico 87545
(Received 18 July 1990)

Reflectance studies on single crystals of a series of rare-earth (R = Pr, Nd, Sm, Gd) copper oxides have been made to determine phonon frequencies as a function of rare-earth mass. The increase in interatomic force constants with increasing rare-earth mass, which leads to a reduction in the lattice parameters, increases the vibrational frequencies. In addition, the change from the T-phase La_2CuO_4 to the T'-phase R_2CuO_4 crystal structure causes changes in the phonon frequencies that are due both to the changing lattice parameters and to the relocation of the apical oxygen atoms.

I. INTRODUCTION

The recent discovery of n-type superconductors in lanthanide copper oxides[1,2] has brought renewed interest to the optical characterization of these materials.[3] There is a structural phase change in the lanthanide cuprates when La is replaced by Pr, Nd, Sm, or Gd.[4,5] These structural changes have a direct effect upon the phonon frequencies in the ir spectrum and, knowing the phonon assignments for the La compound,[6–10] the assignments for the substituted compounds can be made by a direct comparison.[11] This paper will discuss the effects of the different rare earths on the crystal structure and how these changes affect the phonon frequencies. Infrared ab plane reflectance will be analyzed for the frequency shifts due to the relocation of the apical oxygen atoms. An estimate of the zero-frequency dielectric constant will be made from two separate calculations. Our results are in good agreement with recent studies of Nd_2CuO_4 (Refs. 6 and 12) and Pr_2CuO_4.[13,14]

These materials form in a tetragonal crystal structure, when R is one of the rare earths Pr through Gd, with CuO_2 planes in which the oxygen atoms are square-planar coordinated about copper ions.[4,5,15] Unlike the orthorhombic (quasitetragonal) La_2CuO_4, where the CuO_4 are octahedral coordinated with two apical oxygens, the apical oxygen atoms have relocated to form an R-O_2-R plane between the CuO_2 planes. This allows for a more compact structure and the unit-cell volume decreases monotonically with increased R mass (i.e., decreased R ionic size),[5] as shown in Fig. 1(a).

Phonon assignments can be made by using a simple harmonic-oscillator model incorporating the changing structural parameters. The phonon center frequency is $\omega_0=(\kappa/\mu)^{1/2}$, where κ is an effective force constant between the atoms and μ is the reduced mass of the participating atoms. Both force constant and mass change with rare earth. In Fig. 1(b) nearest-neighbor distances, D_{NN}, for the pure lanthanide compounds[16] are plotted versus R mass and show decreasing interatomic distances with increasing mass. This implies that the force constant will grow larger with increasing mass. At the same time, the apical oxygen atoms are pushed from their octahedral coordination above the copper atoms to positions on the unit-cell faces and are sandwiched in between the rare-earth atoms to form an R_2O_2 plane (T to T' phase).[1,15] The consequence of this structural change [Figs. 1(c) and 1(d)] is that the c axis becomes shorter and the a axis broadens out, going from a long and thin unit cell to a short and wide unit cell.[5]

Four in-plane infrared-active (E_u) modes have been identified in the La_2CuO_4 compound.[6–10] It would be expected that three of these modes (the CuO_2 stretch, the CuO_2 bending, and the R-lattice modes) would change in accordance with the lattice parameters, while the mode associated with the apical oxygen bending should disappear and be replaced by a higher-frequency mode of the R_2O_2 in-plane vibration.

II. EXPERIMENT

Single crystals and polycrystalline ceramic pellets were made at the University of Florida and at Los Alamos National Laboratories using techniques which have been described elsewhere.[17] The optical measurements reported in this paper were performed on flakelike crystals and ceramic pellets without after-synthesis polish. We attempted to dope one Nd_2CuO_4 ceramic sample and the

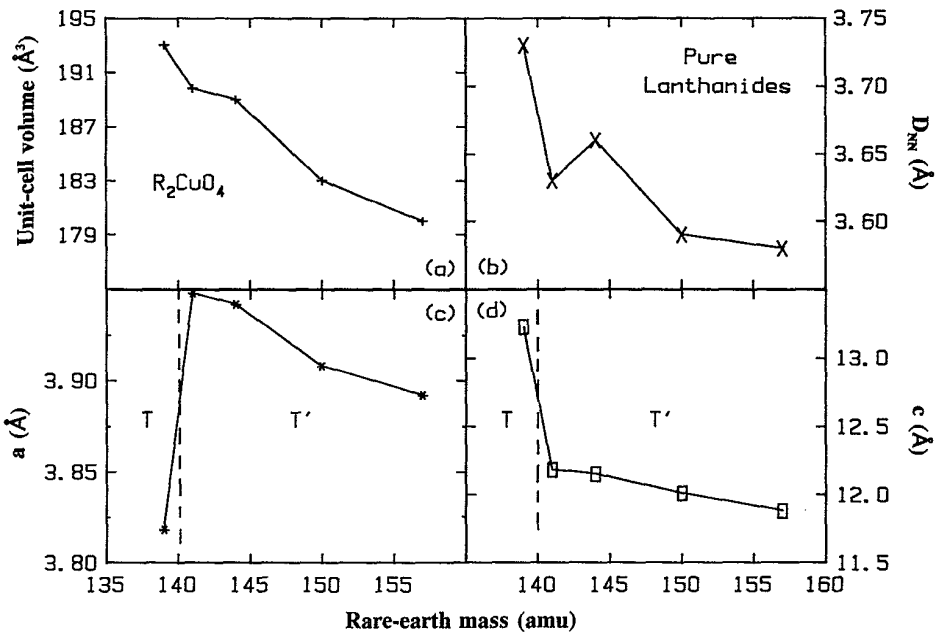

FIG. 1. Lattice parameters for lanthanide compounds, (a) the unit-cell volume (Ref. 5), for R_2CuO_4, (b) the nearest-neighbor distance for the pure lanthanide materials (Ref. 16), (c) and (d) the *a*- and *b*-lattice constants for the R_2CuO_4 compounds (Ref. 5) respectively, as a function of R mass.

Nd_2CuO_4 crystal with Sr^{2+}; however, as Sr^{2+} doping has no effect on the electrical or optical properties, it is evident that Sr^{2+} does not enter the crystal structure. Hence, these samples are equivalent to the undoped insulating compound and we will refer to them as undoped.

Reflectance measurements were taken on a Bruker 113V FTIR interferometer for the ir region from 50–5000 cm^{-1} (0.0062–0.62 eV) and with a homebuilt grating spectrophotometer based on a Perkin-Elmer monochromator over 1000–32000 cm^{-1} (0.12–4 eV). In order to correct for scattering losses due to surface features and/or roughness, the samples were coated with a thin layer (2000 Å) of aluminum. The aluminum-coated spectra, along with the known reflectance of aluminum, were used to correct the sample spectra.

III. RESULTS AND DISCUSSION

A. Reflectance and optical constants

Figure 2 shows the reflectance data for three single crystals and two pellet samples for a series of rare-earth substitutions with the curves offset for ease of viewing. (Note: The Nd_2CuO_4 crystal was the sample which we unsuccessfully attempted to dope with Sr^{2+}.) The plots are limited to data below 1000 cm^{-1} in order to show the phonon region more clearly. Figure 3 shows the entire frequency range up to 32 000 cm^{-2} (4 eV) for two crystals. These compare well to features that have been reported by Cooper *et al.*[14] and Tokura *et al.*,[18] with insulating behavior in the mid-ir and a charge-transfer peak at 12 000 cm^{-1} (1.5 eV).

Returning to the low-frequency spectra, we note that the double peak in the Gd_2CuO_4 spectra near 100 cm^{-1} is associated with a signal-to-noise problem due to small sample size and is actually a single peak. This noise results in large error bars in the exact position of this peak (± 7 cm^{-1}). Secondly, there are additional features in the pellet sample spectra (shoulders near 140, 280, and 550

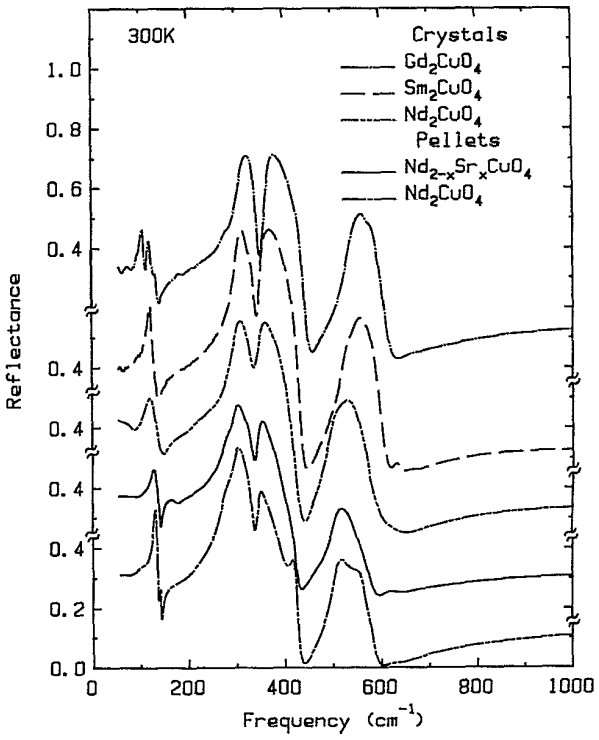

FIG. 2. Infrared reflectance for three single crystals and two pellet samples for a series of rare-earth substitutions (the curves have been offset by a constant for ease of viewing).

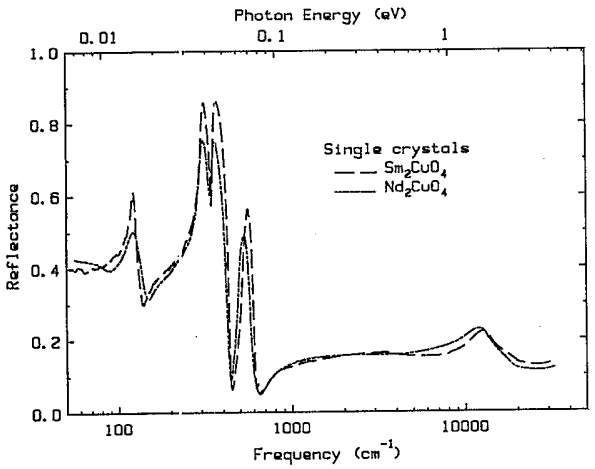

FIG. 3. Reflectance in the infrared and visible for crystals of Sm_2CuO_4 and Nd_2CuO_4.

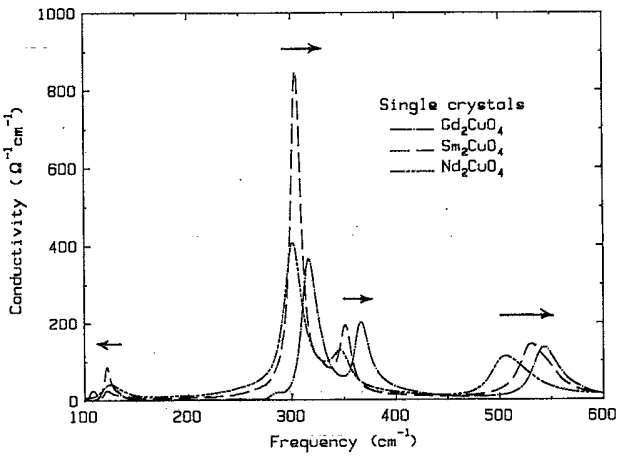

FIG. 4. Frequency-dependent conductivity for crystal samples as obtained from Kramers-Kronig analyses. Arrows indicate shift direction with increasing R mass.

cm^{-1}) which are most likely due to c-axis phonons in these randomly oriented samples.[12,13] The origin of the feature at 404 cm^{-1} in the Nd_2CuO_4 pellet spectra is unknown.

The phonon frequencies can be seen much more clearly by performing a Kramers-Kronig analysis and examining the real part of the frequency-dependent conductivity, $\sigma_1(\omega)$, as shown in Fig. 4. As the rare-earth mass increases, phonons above 300 cm^{-1} shift to higher frequencies while the one below 300 cm^{-1} shifts to lower frequencies (indicated by arrows). Comparison of $\sigma_1(\omega)$ for the pure Nd and doped NdSr pellet compounds (not shown here) finds no differences in the in-plane phonon frequencies, which indicates that no doping took place, i.e., $x=0.00$ for all Nd samples.

B. Phonon frequencies

The phonon frequencies can be determined from the maxima in $\sigma_1(\omega)$, but we have also used a fit to a model dielectric function consisting of four Lorentz oscillators plus a core dielectric constant ϵ_∞ due to higher-frequency contributions

$$\epsilon(\omega)=\sum_{i=1}^{4}\frac{\omega_{pi}^2}{\omega_i^2-\omega^2-i\gamma_i\omega}+\epsilon_\infty ,$$

which is then used to calculate $\sigma_1(\omega)$,

$$\sigma_1(\omega)=\frac{\omega}{4\pi}\mathrm{Im}[\epsilon(\omega)] .$$

This is then fit to the data using a nonlinear-least-squares-fitting routine. Fit parameters are listed in Table I for the single-crystal samples.

Figure 5 has four panels plotting the center frequency as a function of rare-earth mass for each of the in-plane ir active modes. Data for Pr by Crawford *et al.*[13] and for La by Collins *et al.*[8] is also shown. In Figs. 5(b), and 5(d), the CuO_2 stretching and bending modes show a sharp decrease in photon frequency from the T to the T' phase, followed by a frequency increase with increasing R mass. This behavior is just the inverse of the a lattice parameter [Fig. 1(c)] and shows that the Cu-O force constant is increased by the a-axis contraction. A new high-frequency mode in Fig. 5(c) near 350 cm^{-1} appears that is due to the R_2O_2 mode in the T' structure and replaces the 168 cm^{-1} apical bending mode in the T structure. This mode has similar behavior to the CuO_2 bending and stretching modes in the T' phase. The final mode near 125 cm^{-1}, which is associated with the R-lattice vibration in the T phase, is shown in Fig. 5(a). Here we see that the relationship with the changing a-lattice parameter is very weak. However, the gradual shift allows us to retain the mode assignment. There is a shift down in frequency when La is changed to Pr (T to T' phase), which is due to the relocation of the apical oxygens into a tighter formation around the rare-earth ions. Further

TABLE I. Parameters for Lorentz oscillator fits to the frequency-dependent conductivity.

	Nd_2CuO_4			Sm_2CuO_4			Gd_2CuO_4	
ω_i	ω_{pi} (cm^{-1})	γ_i	ω_i	ω_{pi} (cm^{-1})	γ_i	ω_i	ω_{pi} (cm^{-1})	γ_i
127	308	51	123	210	9	121	170	20
301	732	23	304	790	12	318	615	17
346	392	26	351	406	16	368	468	20
510	524	42	534	539	35	545	499	31
	$\epsilon_\infty=5.0$			$\epsilon_\infty=6.5$			$\epsilon_\infty=6.0$	

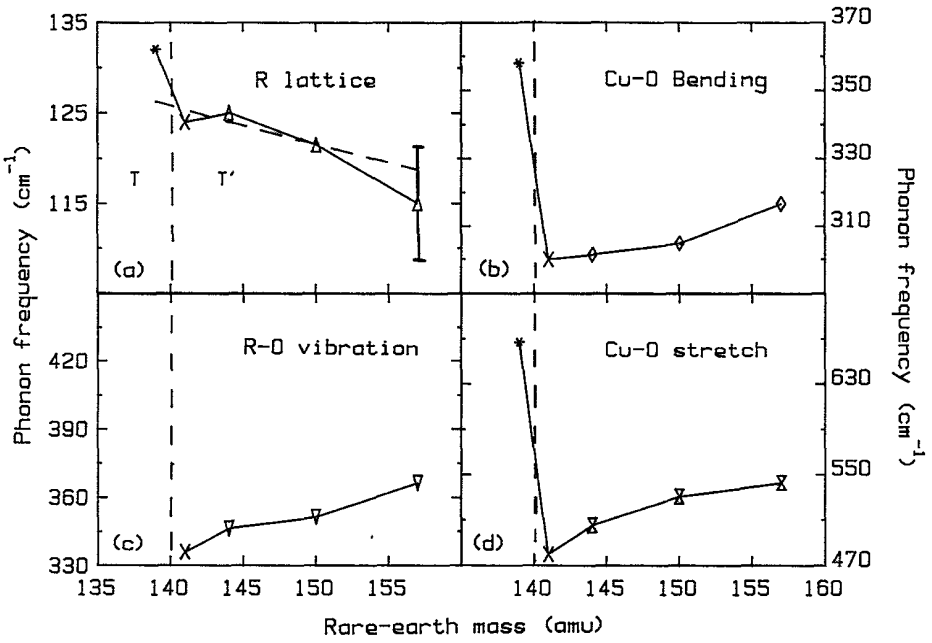

FIG. 5. Center frequency as a function of rare-earth mass for each of the in-plane ir active modes at room temperature. Data for Pr (T=10 K) by Crawford *et al.* (Ref. 13) (×) and for La (T=300 K) by Collins *et al.* (Ref. 8) (*) is also shown.

softening of the mode with Nd, Sm, and Gd substitutions is probably due to the increased mass of the ions. The dashed line in Fig. 5(a) represents the calculated shift in frequency due to simple mass substitution with no change in the force constant (using Sm as the reference for Pr, Nd, and Gd). The agreement between Pr, Nd, and Sm is quite good and the calculated value for Gd falls within the experimental error bars, which is consistent with this picture.

C. Dielectric constant

In addition to the phonon frequencies, we are interested in their intensities or oscillator strengths, because the oscillator strengths govern the zero-frequency dielectric constant $\epsilon_0=\epsilon_1(\omega=0)$. Two estimates of these quantities were utilized: (1) the real part of the frequency-dependent dielectric function as calculated from the Kramers-Kronig analyses, and (2) fits to the real part of the frequency-dependent conductivity using a model dielectric function. The real part of the dielectric function $\epsilon_1(\omega)$ is plotted in Fig. 6 with the zeros offset for comparison. Linear extrapolations to zero frequency result in the values listed in Table II as $\epsilon_1(0)_{\text{expt}}$. From the oscillator-fit parameters, the contributions of the individual phonons are calculated as the square of the oscillator strength over the center frequency $\Delta\epsilon_i=(\omega_{pi}/\omega_i)^2$. The dielectric constant is the sum of these contributions plus ϵ_∞ or

$$\epsilon_0=\sum_{i=1}^{4}\Delta\epsilon_i+\epsilon_\infty\ .$$

Table II lists the results of this calculation showing the phonon contributions, the core dielectric constant, and the sum of these contributions. The phonon-oscillator strengths contribute a large portion of the overall zero-frequency dielectric constant as compared to the core dielectric contribution. The results of both the extrapola-

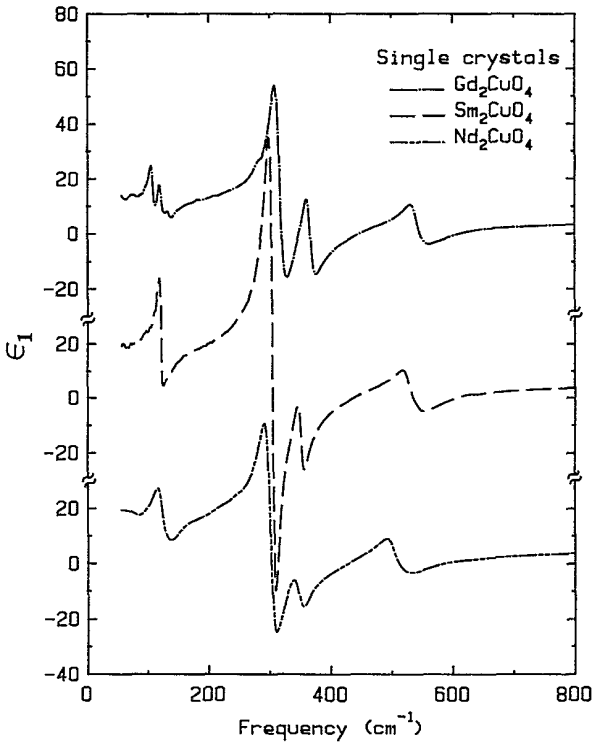

FIG. 6. The real part of the dielectric function $\epsilon_1(\omega)$ for single-crystal samples plotted with the zeros offset for ease of comparison.

TABLE II. Phonon and core dielectric contributions to the zero-frequency dielectric constant as determined by fits to the frequency-dependent conductivity. The sums of these are compared to the experimental values obtained by extrapolation of the real part of the dielectric function to zero frequency.

	$\Delta\epsilon_i=(\omega_{pi}/\omega_i)^2$						
	$i=1$	2	3	4	ϵ_∞	$\sum\Delta\epsilon_i+\epsilon_\infty$	$\epsilon_1(0)_{\text{expt}}$
Nd_2CuO_4	6.0	5.9	1.3	1.1	5.0	19.3	19.3
Sm_2CuO_4	2.9	6.8	1.3	1.0	6.5	18.5	19.5
Gd_2CuO_4	2.0	3.7	1.6	0.8	5.9	14.0	13.5

tion and the fit estimates are consistent with dielectric constants that are rather high for ionic crystals but not excessively so [compare Al_2O_3 at $\epsilon_1(0)\approx 10$]. These values compare well with similar estimates in the T' compounds.[12,13] Note that the ab plane $\epsilon_1(0)$ is about a factor of 2 smaller than the result of Collins *et al.*[8] for La_2CuO_4 but quite close to what Mostoller *et al.*[6] found in single crystal La_2CuO_4.

IV. CONCLUSIONS

In summary, the apical bending mode of the T-phase structure (168 cm^{-1}) is absent in the T'-phase structure and is replaced by a higher-frequency mode at $\sim$350 cm^{-1} due to the R_2O_2 plane vibrations. This is due to the relocation of the oxygen atoms between the R atoms in the T' structure. This mode, along with the CuO_2 stretching, $\sim$550 cm^{-1}, and bending, $\sim$310 cm^{-1}, modes behave as predicted, having an inverse relationship with the a-lattice parameter. The lowest-frequency mode, $\sim$125 cm^{-1}, due to the R-lattice vibration softens only slightly upon rare-earth substitution. The continued softening of this mode results directly from the increased masses in Sm and Gd. Finally, the measured dielectric constant is larger than many ionic materials; however, it is not as large as ferroelectric materials, indicating that these materials are not ferroelectrics.[19]

ACKNOWLEDGMENTS

This work has been supported, in part, by U.S. Defense Advanced Research Projects Agency (DARPA) Grant No. MDA972-88-J-1006 at the University of Florida, and by the Joseph H. DeFrees Grant of Research Corporation Grant No. C-2943 and VCU Grants-In-Aid Grant No. 90-003 at Virginia Commonwealth University.

*Present address: AT&T Bell Laboratory, Murray Hill, New Jersey 07974.

[1]Y. Tokura, H. Takagi, and S. Uchida, Nature (London) **337**, 345 (1989); H. Takagi, S. Uchida, and Y. Tokura, Phys. Rev. Lett. **62**, 1197 (1989).

[2]J. T. Markert and M. B. Maple, Solid State Commun. **70**, 145 (1989).

[3]For example, S. H. Wang, Q. Song, B. P. Claymen, J. L. Peng, L. Zhang, and R. N. Shelton, Phys. Rev. Lett. **64**, 1067 (1990); S. Sugai, T. Kobayashi, and J. Akimitsu, Phys. Rev. B **40**, 2686 (1989).

[4]Hk. Müller-Buschbaum and W. Wollschäger, Z. Anorg. Allg. Chem. **414**, 76 (1975).

[5]I. S. Shaplygin, B. G. Kakhan, and V. B. Lazarev, Russ. Inorg. Chem. **24**, 6 (1979).

[6]Mark Mostoller, Jiquang Zhang, A. M. Rao, and P. C. Eklund, Phys. Rev. B **41**, 6488 (1990).

[7]G. L. Doll, J. T. Nicholls, M. S. Dresselhaus, A. M. Rao, J. M. Zhang, G. W. Lehmen, P. C. Eklund, G. Dresselhaus, and A. J. Straus, Phys. Rev. B **38**, 8850 (1988).

[8]R. T. Collins, Z. Schlesinger, G. V. Chandrashekhar, and M. W. Shafer, Phys. Rev. B **39**, 2251 (1989).

[9]A. V. Bazhenov, T. N. Fursova, V. B. Timofeev, A. S. Cooper, J. P. Remeika, and Z. Fisk, Phys. Rev. B **40**, 4413 (1989).

[10]L. Pintschovius, J. M. Bassat, P. Odier, F. Gervais, G. Chevrier, W. Reichardt, and F. Gompf, Phys. Rev. B **40**, 2229 (1989).

[11]K. K. Singh and P. Ganguly, Spectrochim. Acta **40a**, 539 (1984).

[12]M. K. Crawford, G. Burns, G. V. Chandrashekhar, F. H. Dacol, W. E. Farneth, E. M. McCarron, III, and R. J. Smalley, Phys. Rev. B **41**, 8933 (1990).

[13]M. K. Crawford, G. Burns, G. V. Chandrashekhar, F. H. Dacol, W. E. Farneth, E. M. McCarron, III, and R. J. Smalley, Solid State Commun. **73**, 507 (1990).

[14]S. L. Cooper, G. A. Thomas, J. Orenstein, D. H. Rapkine, A. J. Millis, S-W. Cheong, A. S. Cooper, and Z. Fisk, Phys. Rev. B **41**, 11 605 (1990).

[15]S-W. Cheong, J. D. Thompson, and Z. Fisk, Physica C **158**, 109 (1989).

[16]C. Kittel, *Introduction to Solid State Physics,* 5th ed. (Wiley, New York, 1976), p. 32.

[17]J. D. Thompson, S-W. Cheong, S. E. Brown, Z. Fisk, S. B. Oseroff, M. Tovar, D. C. Vier, and S. Schultz, Phys. Rev. B **39**, 6660 (1989).

[18]Y. Tokura, S. Koshihara, T. Arima, H. Takagi, S. Ishibashi, T. Ido, and S. Uchida, Phys. Rev. B **41**, 11 657 (1990).

[19]D. Reagor, E. Ahrens, S-W. Cheong, A. Migliori, and Z. Fisk, Phys. Rev. Lett. **62**, 2048 (1989).